NBSIR 81-2293

Mass Spectrometric Studies of MHD Slag Thermochemistry

J. W. Hastie and E. R. Plante

High Temperature Processes Group
Chemical Stability and Corrosion Division
Center for Materials Science
U.S. Department of Commerce
National Bureau of Standards
Washington, DC 20234

June 1981

Interim Report

. DEPARTMENT OF COMMERCE
IONAL BUREAU OF STANDARDS

NBSIR 81-2293

MASS SPECTROMETRIC STUDIES OF MHD SLAG THERMOCHEMISTRY

J. W. Hastie and E. R. Plante

High Temperature Processes Group
Chemical Stability and Corrosion Division
Center for Materials Science
U.S. Department of Commerce
National Bureau of Standards
Washington, DC 20234

June 1981

Interim Report

U.S. DEPARTMENT OF COMMERCE, Malcolm Baldrige, *Secretary*
NATIONAL BUREAU OF STANDARDS, Ernest Ambler, *Director*

Mass Spectrometric Studies of MHD Slag Thermochemistry

J. W. Hastie and E. R. Plante
Chemical Stability and Corrosion Division
National Bureau of Standards

The economic viability of open cycle coal-fired magnetohydrodynamics (MHD) is closely linked to the thermodynamic conditions of seed potassium, both in the plasma and slag phase. Previous attempts to model plasma conductivity and slag retention of seed have been highly inaccurate due to the limited thermodynamic data base available. These limitations have mainly included vapor pressure, enthalpy of formation, and solution activity data for slag phases. Results of an extensive systematic measurement program on these and related properties are presented. The following potassium-containing systems were studied: binary mixtures of K_2O with SiO_2, Al_2O_3, Fe_2O_3, and ZrO_2; a series of more complex synthetic slags containing K_2O, SiO_2, CaO, MgO, Al_2O_3, and Fe_2O_3; an MHD channel slag (Illinois No. 6 coal); and several slag-NaCl mixtures. Data were obtained over a sufficiently wide range of component-type, composition, and temperature to reveal systematic trends in slag activities from which empirical predictions are possible. However, anomalous behavior was also noted, mainly in the form of non-equilibrium and phase-separation effects. Application of the vaporization and activity data to plasma-slag interaction and to the recovery of potassium seed from slag is also considered.

1. Introduction

MHD efficiency is closely coupled to the system thermochemistry and, to a lesser degree, rate processes. The main thermochemical processes underlying MHD occur primarily in the plasma or working fluid, the plasma-wall boundary layer, the wall-slag layer, and in seed recovery processing. Potassium-containing species are key components in each of these process elements, as discussed elsewhere (Hastie et al. 1981a). The present discussion is concerned primarily with slag related thermochemistry.

Maintenance of a slag layer is considered desirable, and perhaps essential, in hot wall open cycle coal-fired MHD systems. Studies of slag deposits and seed absorption in an open cycle coal-fired MHD test generator indicate that about 17 to 20 percent of the potassium seed is bound in the slag at 1400 K (Crawford, et al. 1975). This concentration level is about a factor of three lower than that predicted from equilibrium calculations, assuming K_2SiO_3 and K_2SO_4 as the principle condensed phase alkali species. Only about half of the seed slag is readily recoverable, and this is present as K_2SO_4 adsorbed on the slag surface. The economic benefits expected of MHD will certainly not be realized if seed losses of this magnitude occur (by slag absorption).

Attempts to predict the degree of seed-slag interaction for various coal types and operating conditions have suffered greatly from the complete lack of potassium-enriched slag activity and related phase equilibria data. Efforts to simulate the non-ideality of slag in thermochemical calculations have been made by assuming ideal solutions of known compounds, such as $Al_6Si_2O_{13}(\ell)$, $SiO_2(\ell)$, $Al_2O_3(\ell)$, $FeO(\ell)$, $K_2SiO_3(\ell)$, etc. (Spencer and Orning, 1973; Hsu and Johnson, 1979). However, these thermodynamic models have proved to be less than satisfactory in the prediction of seed-slag retention (Spencer et al. 1975).

Bench scale tests and thermodynamic calculations indicate the feasibility of seed recovery from the K_2SO_4 phase, although the crude estimates used for K species thermodynamic data contributed to appreciable differences between observed and calculated product yields (Materi, 1978). Given the high absorptivity of coal slag for K_2O from the plasma phase, seed recovery from slag also appears desirable, though no thermochemical schemes have been developed.

The present work addresses these questions of slag activities and seed absorption thermochemistry, together with the problem of seed recovery from potassium silicate slag phases. The primary experimental methods used in this study are the Knudsen Effusion Mass Spectrometric (KMS) and Transpiration Mass Spectrometric (TMS) methods, as described elsewhere (KMS, Plante, 1979a; TMS, Bonnell and Hastie, 1979). Both are modulated molecular beam methods, with phase sensitive detection, and they allow for accurate measurement of both gaseous and condensible species. These techniques also provide a unique capability for in-situ determination of condensed phase composition in non-congruent vaporizing systems. The basic differences between the KMS and TMS methods are the upper pressure limits of 10^{-4} and one atm,[1] respectively, and upper limit gas residence times of about 0.04 and 20 sec, respectively. Thus, the TMS method will more closely approach the equilibrium condition for systems exhibiting non-equilibrium behavior.

2. Synthetic Slag Systems

2.1 Background

As part of a program of systematic studies on potassium-containing slag systems, vaporization data have been obtained for a series of synthetic-binary, ternary, quarternary and sexternary oxide mixtures, as well as an actual MHD coal-slag sample. Virtually no experimental thermodynamic activity data exist for these systems. Even for the most studied relatively simple K_2O-SiO_2 system, existing data are extremely crude and incomplete. Comparison of our results with those reported by Charles (1967), as based on the moist-atmosphere transpiration data of Preston and Turner (1933), indicate order-of-magnitude differences, with the Charles's activities being low.

Table 1 contains a summary of selected potassium vaporization data for these systems. With a few noted exceptions, the oxygen partial pressures coupled stoichiometrically with potassium, in keeping with the process,

$$K_2O(\ell) = 2K + 1/2\ O_2 \quad . \qquad [1]$$

Hence, $K_2O(\ell)$ activities can be derived, to a good to excellent approximation, using the corresponding dissociation pressure data for pure liquid K_2O. That is,

$$A_{K_2O} = (P_K)^{5/2}/2K_p \quad , \qquad (1)$$

---

[1] 1 atm = 1.01325×10^2 kpascal.

where K_p is the dissociation constant for pure liquid K_2O. We have derived a temperature dependent expression for K_p as follows. From JANAF (1971), K_p data for $K_2O(s)$ are available. Combining these results with the fusion enthalpy and entropy data of Natola and Touzain (1970), and an estimated C_p for liquid K_2O of 25 cal/deg mol, leads to the expression,

$$\log K_p\ [K_2O(\ell)] = \frac{-23751}{T} + 11.7723 \quad .$$

The potassium vapor pressure data were obtained under neutral conditions using the TMS technique. For most MHD conditions of interest, iron will be present in the slag as Fe_3O_4. Hence the data reported in table 1 were obtained, for the most part, at temperatures (and run times) where Fe_2O_3 (slag) had essentially converted to Fe_3O_4 (slag). This reduction was conveniently established by monitoring the O_2-pressure. These results can also be applied to systems where O_2-sources other than reaction [1] are present. In this case, the K-pressures are converted to activities using equation (1). The activity data are then combined with the known equilibrium constant for reaction [1], and the assigned O_2-pressures, to yield the new K-pressure data. For relatively low temperature oxidizing conditions, where Fe_2O_3 (slag) may be present, we can reasonably assume that the present activity data will be valid. That is, the various forms of iron oxide do not significantly affect the alkali activity.

Experimental details and an extended discussion of these potassium vapor pressure results have either appeared, or will appear, elsewhere, as indicated in table 1. In general, the potassium vaporization data followed the expected Clausius-Clapeyron behavior, as indicated in table 1. Exceptions to this behavior could be traced to:

(a) residual alkali carbonate impurities resulting either from the sample synthesis method, or from condensation out of MHD plasmas with actual slag samples;

(b) non-equilibrium effects in the condensed phase;

(c) non-equilibrium between the condensed and vapor phase leading to an unsaturated vapor;

(d) changing phase boundaries due to incongruent vaporization;

(e) rapid loss of alkali pressure with time (T constant), possibly, resulting from surface depletion in highly viscous systems; and,

(f) Fe-controlled redox reactions resulting in changing oxygen and, hence, K-partial pressure data with temperature and time.

A systematic study of systems with a progressive increase in the number of components was necessary to isolate and quantify such behavior. Some of these exceptional cases are discussed as follows.

2.2 K_2O-Al_2O_3-SiO_2 System

The K_2O-Al_2O_3-SiO_2 system has the potential for forming several stable or metastable phase assemblages in which the K_2O activity is fixed according to the phase rule (see table 1). However, in practice, we observe the K-pressure (and hence K_2O activity) to be dependent on bulk composition. This effect could result from several non-equilibrium factors including, slow condensed phase kinetics attributable to the complex crystal chemistry, changing composition in the β-alumina phase (which extends from K_2O/Al_2O_3 ratios of 1/5 to 1/9), or to dissolution of SiO_2 in the β-alumina phase. The vapor pressure equation in table 1, for the three phase region, is based on the highest alkali-pressures which were effectively independent of composition.

Other evidence for non-equilibrium behavior is shown in figure 1. In the previous experimental run, alkali-pressure data were obtained as a function of increasing temperature up to 1860 K. On decreasing the temperature, lower pressures were found than for the increased-temperature run, particularly at 1760 K and below. As shown in figure 1, continuation of this experiment initially produced low pressures over the AB interval. The temperature and K_2O concentration at which this phenomenon was noted is reasonably consistent with the phase diagram which shows eutectic melting at 1829 K and 22 wt.% K_2O (Levin et al., 1964). We attribute this loss of alkali-volatility to formation at the sample surface of a frozen eutectic melt which is probably glassy in nature. For an equilibrium system, this melt would recrystallize but for the present experimental conditions there was probably insufficient time. The phase being depleted by vaporization is $KAlSiO_4$ and the pressure-loss results from the slow alkali transfer rate across the frozen eutectic which results in partial isolation of the remaining $KAlSiO_4$. Note, in figure 1, the upward curvature of the AB interval with increasing temperature. This unusual behavior probably results from remelting of the eutectic barrier phase with an increased rate of alkali transport through this barrier together with incorporation of additional $KAlSiO_4$ in the eutectic melt.

2.3 K_2O-CaO-Al_2O_3-SiO_2 System (Simplified "Western" Slag)

These four component systems, designated as Simplified "Western" Slags in table 1, are relatively well behaved in terms of alkali vaporization and are useful model systems for sub-bituminous basic coal slags (as discussed in Section 2.5). The data have been cast in analytical form, as summarized in table 1.

2.4 K_2O-CaO-MgO-Al_2O_3-Fe_2O_3-SiO_2 System (Synthetic MHD Channel Slags of "Eastern" and "Western" Coal Types)

Literature compositional analyses of several hundred coal ash and several MHD channel slags, containing potassium seed, have been evaluated for the purpose of selecting representative compositions for modeling. Table 1 indicates the compositions selected as most representative of MHD channel slags of "Eastern" and "Western" coal types. These slags are non-glassy with $KAlSiO_4$ (kalsilite) as the dominant crystalline phase (in both slag types) and small amounts of $KAlSi_2O_6$ and at least one unidentified phase (for "Eastern" slag type only). Thus the bulk composition is not as meaningful a variable as for glassy slags. Vapor pressure measurements were made using a relatively small effusion orifice (0.34 mm diameter) to reduce the possibility of vapor unsaturation found earlier on similar mixtures but with larger orifices (0.5 to 1.0 mm). Steady state pressures were not obtained until about ten percent of the K_2O content had been depleted by vaporization. Excess oxygen was vaporized during this initial experimental phase with reduction of FeO_x ($x = 1.5$ to 1.33). Following this initial reduction period, the oxygen partial pressure was, within experimental error, what would be expected if the O_2 pressure were controlled by K_2O dissociation.

Figure 2 compares vapor pressure data for the "Western" and "Eastern" slags. This comparison clearly demonstrates a basic difference between "Western" and "Eastern" slags in that "Eastern" slags require about twice as much K_2O-content to achieve similar alkali pressures as for "Western" slags. This effect results from the higher concentration of basic CaO and MgO in "Western" slags, leading to a less complex silicate structure in the "Western" slag and, hence, a less bound form of K_2O.

The vaporization behavior of the "Eastern" slag, in the composition range 24 to 21 wt.% K_2O, is very different to that for the "Western" slag, as shown in figure 3. Here, the vapor pressure curves show a significant break at location X, the position of which depends on the amount of sample vaporized. Note the significant positive deviation of the observed K and O_2-pressures (XC interval) from those obtained by extrapolating the higher temperature linear portion of the respective curves. The curves labeled AB in figure 3 were obtained prior to the curves labeled BC. At temperatures above 1620 K, these two curve sets are seen to merge into a single linear portion. This behavior is attributed to a changing oxygen potential in the slag. At the higher temperatures, the oxygen partial pressures were greater than would be predicted by K_2O dissociation alone. However, at the lower temperatures, less oxygen was observed than expected for K_2O dissociation. Apparently, FeO_x undergoes reduction at temperatures above 1620 K with release of additional O_2 (above the K_2O level). Below this temperature, FeO_x is oxidized by the O_2 resulting from K_2O dissociation. It is particularly noteworthy that the K_2O activities derived from these K and O_2-partial pressure data yield a single linear curve over the whole AB, BC intervals (not shown here) as is to be expected for a system at thermodynamic equilibrium. Thus the alkali-partial pressures readily adjust to the perturbing influence of FeO_x redox reactions. It is also significant that these non-linear effects were not noted in the "Western" slags owing to their lower FeO_x content.

2.5 Synthetic Low Melting Slag (K_2)

The K_2-labeled six component slag (see table 1) is not representative of any particular coal type but was formulated to provide a wide liquidus range (1480 K and higher) for detailed solution studies. Comparison of the K_2-slag partial pressure data with that for the relatively simple four component "simplified Western slag" is particularly informative. If we assume, on a molar basis, that Fe_2O_3 (or Fe_3O_4) can be replaced by Al_2O_3 and, likewise, MgO by CaO, then the K_2 slag (6 wt.% K_2O) can be represented in the "simplified Western slag" form of (wt.%) SiO_2 (48.8), Al_2O_3 (19.6), CaO (25.4) and K_2O (6.2). A comparison of the K_2O dissociation pressure curve calculated for this composition (see table 1) with the directly measured data for the K_2 slag is given in figure 4. Note the good agreement (within 50 percent in K-pressure) between both slag systems, which verifies the molar interchangeability approximation for Fe_2O_3(or Fe_3O_4)-Al_2O_3 and MgO-CaO. Comparable agreement was found for other synthetic and real slag systems, provided CaO was a significant component. Thus, the four component "Simplified Western" synthetic slag system can probably be used to model real slag compositions, at least of the "Western" or basic type.

3. Real MHD Channel Slag (K_1)

Detailed TMS and KMS studies were made of vapor transport over a high liquidus temperature (∿ 1700 K) potassium-enriched coal slag with an initial composition as indicated in table 1. This slag sample was obtained from combustion of Illinois No. 6 coal with additional potassium added to the combustor (see Hastie et al., 1980). For identification purposes, this slag is given the designation K_1. X-ray diffraction data indicated that the bulk of the potassium in the slag was present as the compound $KAlSiO_4$. TMS analysis indicated that about two percent of the potassium was present in relatively volatile form, mainly as K_2SO_4 and K_2CO_3. After depletion of these components by vaporization, the only significant slag vapor species were K and O_2, and these were present in the approximate stoichiometric ratio expected for K_2O decomposition. Hence the FeO_x component was present primarily in reduced form.

Since the mole fraction of K_2O can be defined at any stage of an experiment by integrating the K and O_2 partial pressure data with time, it is possible to convert K-partial pressures to K_2O activity coefficients using equation (1). By varying the amount of K_2O present in the slag during a vaporization run, we were able to follow the dependence of the K_2O "apparent" thermodynamic activity on temperature and composition. The term "apparent" is used to emphasize that the slag system may not always be in a state of complete thermodynamic equilibrium. Typical data, expressed in activity coefficient form [$\gamma(K_2O)$], are given in figure 5. Most of these data were obtained below the liquidus temperature. Good agreement was obtained between the TMS and KMS-based data at relatively high temperatures (∿ 1600 K). From this observation, we can conclude that the high temperature data represent thermodynamic equilibrium because of the greatly different residence time scales involved, i.e., TMS ∿ 10 sec and KMS ∿ 0.04 sec.

Note in figure 5, the non-monotonic nature of the activity coefficient curves. For normal non-ideal solution behavior, we would expect a linear monotonic relationship with a negative slope representing a negative excess partial molar enthalpy of solution for K_2O in the slag. This type of behavior occurs for segments of each run (see fig. 5), e.g., for run 1, up to about 1430 K, and for run 2 between 1430 and 1630 K. However, the run 1 data are anomalous as they were obtained during the initial heating period when K_2SO_4 and K_2CO_3 decomposition was a significant source of additional K. The rapid reduction in $\gamma(K_2O)$ as the temperature is increased beyond 1430 K, results from the virtually complete depletion of these relatively volatile forms of potassium. For runs 2 and 3, the initial reduction of $\gamma(K_2O)$ with increasing temperature is believed to be due either to diffusion limited (in solid slag) K-transport to the slag surface or to changes in the mode of O_2 release from the slag, for instance through Fe_3O_4 dissociation. The onset of increasing $\gamma(K_2O)$ with temperature is believed to arise either from an as yet unspecified physiochemical change in the slag, leading to a less viscous (but still solid) form and increased diffusion, or to depletion of secondary O_2 sources. At higher temperatures, the bulk composition changes rapidly (see mole fractions in fig. 5) and leads to a peaking in $\gamma(K_2O)$. We believe that the data for runs 2 and 3, at temperatures in excess of 1450 K, represent an equilibrium vaporization condition, particularly as the KMS and TMS data are in agreement for these conditions. Clearly, these unusual trends in the $\gamma(K_2O)$ data indicate the difficulty involved in making a priori predictions of real slag vaporization behavior.

4. Application of Vaporization Data to Seed-Slag Interaction

A key factor for successful MHD operation is the degree of interaction between plasma potassium seed and the slag medium. Using slag activity data from the present studies, it is possible to predict conditions under which plasma seed will be continuously depleted by slag absorption of alkali. Plante et al. (1975) presented similar arguments earlier based on their data for the binary oxide systems. A more definitive analysis can now be made from the present data on complex synthetic and actual slag systems.

The stability of K_2O in slag solutions can be readily determined by comparison of the K_2O dissociation pressure-product $(P_K{}^2 \cdot P_{O_2}{}^{1/2})$ data in the slag phase with that in the plasma phase, as shown in figure 6. This dissociation pressure (DP) expression is a convenient representation of slag activity data [activity = DP, soln/DP, $K_2O(\ell)$]. The DP curves for the plasma phase were calculated using a multicomponent equilibrium computer program, assuming stoichiometric combustion of $CH_{0.7}$ with air (4/1 mole ratio N_2/O_2) and KOH, K, KO and K^+ as vapor phase alkali species. Pressures of ten atm and one atm were chosen to be representative of the MHD combustor and the channel-diffuser-downstream seed recovery units, respectively. Corresponding curves for the simplified "Western" slags were calculated from the experimental vapor pressure data given in table 1.

Comparison of the DP durves (see fig. 6) for plasma and slag indicate interface temperatures for K_2O slag saturation in the range of 2100 to 2500 K at 10 atm and 1900 to 2200 K at 1 atm for the 5 to 15 wt.% K_2O compositions. Experimentally, these interface temperatures are difficult to measure though the data reported by Self (1979) indicate that they are probably in the region of 2100 to 2300 K. Hence, slags of about 10 wt.% K_2O would be present under these conditions. Note that the DP equivalence temperatures in figure 6 are significantly lower for the one atm conditions characteristic of downstream units. Also, as the temperature decreases, the slag DP curves decrease much faster than for the plasma, resulting in a super-saturated alkali vapor concentration at the plasma-slag interface. Therefore, excess seed will tend to deposit on the slag surface in a relatively non-bound form, such as the alkali sulfate or carbonate, which is desirable from a seed-recovery point of view. As the temperature decreases, the reduced slag species diffusion rates and the increased tendency for phase separation will allow these K_2SO_4 and K_2CO_3 deposits to remain at, or near, the slag surface, as is found in practice. On the other hand, the K_2O absorbed at the higher temperatures will remain in the bulk silicate structure on cooling and will be relatively inaccessible to seed recovery processing.

5. Salt-Slag Alkali Exchange

5.1 TMS Study in Salt Liquidus Region

The possibility of NaCl-K_2O (slag) interaction to produce KCl-Na_2O (slag) could greatly enhance release of K to the vapor phase. In MHD slags, where about 20 wt.% K_2O content is possible, the problem of recovering this lost seed could be resolved through replacement by NaCl. The feasibility of such an exchange process was tested by a TMS monitoring of the vapor phase over the system, NaCl + K_1 slag (19.4 wt.% K_2O). Details of this study will be given elsewhere (Hastie et al., 1981b), but the main observations are as follows.

When a thin layer of powdered NaCl was present on the surface of the K_1 slag, a rapid exchange reaction occurred near the melting point of NaCl, i.e.,

$$\mathrm{NaCl}(\ell) + \mathrm{K_2O}\ (\mathrm{slag}) = \mathrm{KCl}(\ell) + \mathrm{Na_2O}\ (\mathrm{slag}) \quad .$$

This result is demonstrated in figure 7, where the observed partial pressures of NaCl and KCl are expressed in thermodynamic activity form. Note the marked decrease in NaCl activity and concomitant increase in KCl activity just above the melting point of NaCl. After a heating period of about 50 min., the NaCl sample was virtually depleted, as was the KCl product. Insufficient salt was present in the initial mixture to convert all the available K_2O to KCl. However, 90 percent of the initial NaCl was converted to Na_2O (slag) with stoichiometric release of KCl. About six percent of the available K_2O was converted to KCl vapor, and we expect that nearly complete removal of K_2O from the slag would have been possible if sufficient NaCl were present. The remaining ten percent NaCl was lost by vaporization before, and during, the exchange process. During the isothermal, constant activity, phase of the exchange process (20 to 40 min. region of fig. 7), a potassium vapor transport enhancement factor of,

$$\frac{P_{KCl}}{P_K \text{ (no NaCl)}} \sim 10^4$$

was observed. Also, during this period, the high KCl activity suggests formation of an essentially ideal solution of KCl-NaCl. Note the near unit NaCl activity in the initial phase of the experiment (fig. 7), which confirms the calibration factors used to convert mass spectral ion intensities to partial pressures and reflects establishment of thermodynamic equilibrium.

5.2 KMS Study in Salt Solidus Region

A very effective exchange between molten NaCl and K_2O (slag) for a high potassia MHD channel slag was indicated by the TMS observations (Section 5.1). An effort to determine the effectiveness of this process in the solid state, and for lower K_2O-slag content (K_2 slag of table 1), was made using the KMS approach. From a thermodynamic viewpoint, the exchange reaction is more favorable at lower temperatures [$K_p(1000\ K) = 2 \times 10^5$, $K_p(700\ K) = 6.5 \times 10^7$]. However, this thermodynamic gain may be offset by slower kinetics in the solid phase.

The Knudsen cell sample contained the K_2 slag plus a separate top layer of NaCl present as powdered material. A relatively small cell orifice diameter of 0.34 mm was used to provide vapor species residence times of about 40 ms. In contrast to the TMS study, excess NaCl was present to allow for a possible complete removal of K_2O from the slag. If all the slag K_2O was converted to KCl without loss of KCl or NaCl through vaporization, the resulting salt mixture would contain 0.2 mole fraction KCl. From the known KCl-NaCl phase diagram (Scheil and Stadelmaier, 1952), such a mixture would form a solid solution in the temperature region of 720 to 1010 K. Mass spectral data were obtained over the temperature range 810 to 1010 K. Only mass spectral ions corresponding to the well known alkali halide species of NaCl, Na_2Cl_2, KCl, K_2Cl_2, and $KNaCl_2$ were observed.

Mass balance considerations indicated a complete conversion of K_2O (slag) to Na_2O (slag) by the halide exchange process. Comparison of the Na_2Cl_2/NaCl partial pressures with the JANAF (1971) values for pure NaCl indicated NaCl activities in the range $\sim$ 1.0 to 0.8 over the whole measurement temperature regime. Moreover, the vapor phase dimer exchange process,

$$Na_2Cl_2 + KCl = NaKCl_2 + NaCl \quad ,$$

(and the corresponding K-case), yielded equilibrium constant, and second and third law reaction enthalpy data in excellent agreement with the literature values (see Hastie, 1971). Thus, thermodynamic equilibrium appears to be established in the overall system.

Several independent sets of thermodynamic KCl activity data were obtained from the KCl and K_2Cl_2 partial pressure data, as shown in figure 8. Note that during the early phase of the experiment, KCl activities as high as 0.62 were present. This is considerably above the maximum value of 0.2 for a thermodynamically ideal solid solution with complete conversion of K_2O (slag) to KCl. However, these data are consistent with the known activity data (see Asano et al., 1980) for the NaCl-KCl system, as shown in figure 8.

The efficiency of potassium transport to the halide phase can be expressed in terms of a distribution coefficient between the slag and halide phases, i.e.,

$$K_D = \frac{X(K_2O),\ \text{slag}}{X(KCl),\ \text{salt}} \quad ,$$

where X is mole fraction. Values of $K_D \sim 0.1$ were found. Similar separation factors have been observed for other metals in borate, rather than silicate, solvent extraction systems (Williams et al., 1977).

These results clearly show the effectiveness of the exchange process under vacuum vaporization and near-atmospheric transpiration conditions. To test whether these observations carry over to static room atmosphere conditions, mixtures of NaCl and K_2 slag were heated in air to 920 K in a muffle furnace. X-ray diffraction analysis of the products showed the presence of both KCl and NaCl solid, but the exchange process appeared to be slower than for the vacuum experiments. It appears possible that the reaction rate is controlled by molecular transport of NaCl vapor to the slag, which would be significantly lower under static atmospheric conditions.

Based on thermodynamic considerations, an analogous even more favorable exchange process should occur with $CaCl_2$. However, exchange between a divalent Ca^{2+} and monovalent K^+ ion may be transport limited and experimental confirmation of this process should be provided.

6. Acknowledgments

A significant portion of this work was supported by the Department of Energy. Mr. Art Sessoms provided valuable technical assistance. Enlightening discussion with Dr. L. Cook is also acknowledged.

Table 1

Summary of Alkali Vaporization Data for K-Containing Complex Oxide and Coal Slag Systems

System[a]	Phases[a,b,e]	Temperature[c] K	K-Pressure[d,e] atm A	K-Pressure[d,e] atm B	Comments[e]
K_2O-SiO_2	Solution 44 to ~ 5[K_2O]	1300-1800	4.721 C = 9.32	15624	Pressures higher than earlier data of Plante et al. (1975) because of orifice effect.
K_2O-Al_2O_3	$KAlO_2 \rightarrow K_2O \cdot 5Al_2O_3$[f]	1300-1800	5.489	15036	P_K independent of bulk composition. Plante et al. (1975).
	$K_2O \cdot 9Al_2O_3 \rightarrow Al_2O_3$[f]	1500-1800	7.487	21453	
K_2O-ZrO_2	$K_4Zr_5O_{12}$-ZrO_2	1100-1450	4.524	12873	Plante (1977).[g]
K_2O-Fe_2O_3	$KFeO_2$-$K_2O \cdot 6Fe_2O_3$[f]	1150-1450	4.524	12873	Phase boundary composition slightly dependent on T. Data adjusted for constant K/O_2. Plante (1979b).
	$K_2O \cdot 6Fe_2O_3$-Fe_3O_4	1200-1600	7.028	16750	
K_2O-Al_2O_3-SiO_2 ($KAlSiO_4$)[h]	$KAlSiO_4$, $K_2O \cdot 9Al_2O_3$, $KAlSi_2O_6$	1400-1650	8.722	20923	Probably not equilibrated because of slow condensed phase kinetics. Plante (1979c, 1980a)
K_2O-Al_2O_3-SiO_2[h]	Possibly $KAlSi_2O_6$, Al_2O_3, $K_2O \cdot 9Al_2O_3$ ~ 22[K_2O]	1600-1900	7.068	20763	Evidence of melt formation.
	Phases uncertain ~ 17[K_2O]	1600-2000	6.350	20693	
	Phases uncertain ~ 11.5[K_2O]	1750-2150	4.667	19800	
	Liquid + $3Al_2O_3 \cdot 2SiO_2$ (10.8[K_2O]) (mullite)	1800-2150	4.464	20424	Decreasing T-chronology used to minimize composition change.

System[a]	Phases[a,b,e]	Temperature[c] K	K-Pressure[d,e] atm		Comments[e]
			A	B	
Simplified Western Slags K_2O-CaO-Al_2O_3-SiO_2	Solution + $KAlSiO_4$ at higher K_2O content	1400-1900	5.228 C = 7.887 exp-2, D = 1.741 exp-3, E = 1.825 exp-2	16794	Composition range, [K_2O] 3-14, [CaO] 17-36, [Al_2O_3] 14-36, [SiO_2]-balance. Standard dev. ~ 30 percent, maximum dev. ~ 100 percent. Additional data for 20[K_2O] compositions have been obtained. Plante (1980a,b,c,d; 1981).
Real MHD Channel Slag (K_1): [K_2O] 19.5, [Al_2O_3] 12.1, [Fe_2O_3] 14.3, [CaO] 3.8, [MgO] 1.0, [SiO_2] 46.8, [Na_2O] 0.5.	$KAlSiO_4$ major + minor unidentified crystalline phase + slag	1600-1800	5.564	16650	Illinois no. 6 coal, UTSI test sample. Initially high pressure of K due to presence of K_2SO_4 and K_2CO_3 (0.2 percent S). Equation corresponds to [K_2O] ~ 14. Hastie et al. (1980).
Synthetic Western Channel slag: [K_2O] 22.7, [Al_2O_3] 24.6, [Fe_2O_3] 5.3, [CaO] 9.3, [MgO] 3.3, [SiO_2] 34.8.	$KAlSiO_4$ + glassy phase	1500-1700	6.818	18472	[K_2O] 18.9-17.6. Plante and Cook (1978).
Synthetic Eastern Channel slag: [K_2O] 23.6, [Al_2O_3] 25.5, [Fe_2O_3] 12.5, [CaO] 1.8, [MgO] 0.6, [SiO_2] 36.0.	$KAlSiO_4$ + glassy phase	1600-1750	6.831	19056	23.3-22.1 [K_2O]. Linear portion of AB, BC curves in figure 3. Plante and Cook (1978).
Illite: [K_2O] 7.4, [Al_2O_3] 26.0, [Fe_2O_3] 4.4, [MgO] 2.1, [SiO_2] 60.2.	Liquid	1550-2085	6.286	20642	Hastie et al. (1979).

System[a]	Phases[a,b,e]	Temperature[c] K	K-Pressure[d,e] atm		Comments[e]
			A	B	
Low Melting Synthetic Slag (K_2): [K_2O] 8.7, [Al_2O_3] 11.1, [Fe_2O_3] 12.0, [CaO] 13.9, [MgO] 7.9, [SiO_2] 47.3.	Liquid	1470-1820	6.231	17863	6[K_2O]. Initial $P_{O_2} \geq P_K$, but later fell to the level of K_2O (see text). Hastie et al. (1980).

---

[a] Initial compositions, given in weight percent (wt.%). Note, actual analyses given not normalized to 100 percent. Fe_2O_3-containing systems usually converted to Fe_3O_4 with loss of O_2 under vacuum or neutral atmosphere vaporization conditions.

[b] Phases indicated are solid.

[c] Temperature range over which experimental data were taken.

[d] Results obtained by KMS. See comments for applicable compositions. Potassium partial pressure data can be represented, to a good approximation, by the empirical form,

$$\log P\ (\text{atm}) = A - B/T + C + D - E \quad ,$$

where A is an entropy term and B is enthalpy; C, D, and E are the factors by which the concentrations (normally in wt.%) of K_2O, CaO, and Al_2O_3, respectively, are to be multiplied. The factor C in the K_2O-SiO_2 system is to be multiplied by the K_2O mole fraction squared. P refers to pressure (atm) of elemental K, as the only K-species present. T is temperature in Kelvin. Other data for individual compositions may be found in the reports cited (see comments). Note, similar data-fits are obtained for compositions expressed in mole %.

[e] Square brackets indicate weight percent composition. Exp-2 denotes, for instance, 10^{-2}.

[f] Exact crystalline phase compositions uncertain.

[g] Pressure could be low by a factor of two because of vapor unsaturation (large orifice). Also, K_2CO_3 contamination present.

[h] Compositions constrained to mole ratio Al_2O_3/SiO_2 = 0.5.

7. References*

Asano, M., Kato, E., and Sato, T. (1980). Mass Spec. Japan 28, 107.

Bonnell, D. W. and Hastie, J. W. (1979). "Transpiration Mass Spectrometry of High Temperature Vapors", in Characterization of High Temperature Vapors and Gases, Hastie, J. W., ed. NBS-SP 561, p. 357.

Charles, R. J. (1967). J. Amer. Ceram. Soc., 50, 631.

Crawford, L. W., Tempelmeyer, K. E., Martin, J., and Muehlhauser, J. (1975). "Investigation of Slag Deposits and Seed Absorption in a Direct-Fired MHD Power Generator". Sixth Intl. MHD Symp., Washington, D.C., June.

Hastie, J. W. (1971). "Thermodynamic Studies by Mass Spectrometry of Molten Mixed Halide Systems" in, Advances in Molten Salt Chemistry, Vol. 1, p. 225, Braunstein, J., Mamantov, G., and Smith, G. P., eds., Plenum Press.

Hastie, J. W., Bonnell, D. W., Plante, E. R., and Horton, W. S. (1980). "Vaporization and Chemical Transport Under Coal Gasification Conditions". NBSIR 80-2178.

Hastie, J. W., Plante, E. R., and Bonnell, D. W. (1979). "Molecular Basis for Release of Alkali and Other Inorganic Impurities from Coal Minerals and Fly Ash". Report to DoE, Morgantown, WV. Nov.

Hastie, J. W., Plante, E. R., and Bonnell, D. W. (1981a). "Alkali Vapor Transport in Coal Conversion and Combustion Systems", NBSIR 81-349.

Hastie, J. W., Plante, E. R., and Bonnell, D. W. (1981b). "Slag-Alkali Halide Exchange Reactions". To be published.

Hsu, C. C. and Johnson, C. E. (1979). "Potassium Seed Activities in Open Cycle MHD Systems: Predictions Using a Multicomponent Solution Model." ibid. Bonnell and Hastie (1979).

JANAF (1971). Joint Army, Navy, Air Force Thermochemical Tables, 2nd Ed., NSRDS-NBS 37. See also later supplements for 1971-1981.

Levin, E. M., Robbins, C. R., and McMurdie, H. F. (1964). Phase Diagrams for Ceramists. p. 407. Am. Ceram. Soc., Columbus, OH.

Materi, G. E. (1978). "An Evaluation of the Direct Reduction Seed Regeneration Process--Topical Report". UTSI, Tullahoma, TN.

Natola, F. and Touzain, Ph. (1970). Can. J. Chem., 48, 1955.

Plante, E. R. (1977). In, Development, Testing, and Evaluation of MHD Materials, H. P. Frederikse, T. Negas, and S. J. Schneider, eds., NBS Quarterly Progress Report to DOE, March.

Plante, E. R. (1979a). "Vapor Pressure Measurement of Potassium Over K_2O-SiO_2 Solutions By a Knudsen Effusion Mass Spectrometric Method". ibid, Bonnell and Hastie (1979).

Plante, E. R. (1979b). In, Properties of Electronic Materials, J. R. Manning, ed., NBSIR 79-1976.

Plante, E. R. (1979c). In, MHD Materials-Seed/Slag Interactions and Effects, S. J. Schneider, ed., NBS Report to DoE, December.

Plante, E. R. (1980a). In, MHD Materials-Seed/Slag Interactions and Effects, S. J. Schneider, ed., NBS Quarterly Progress Report to DoE, March.

Plante, E. R. (1980b). In, MHD Materials-Seed/Slag Interactions and Effects, S. J. Schneider, ed., NBS Quarterly Progress Report to DoE, June.

Plante, E. R. (1980c). In, MHD Materials-Seed/Slag Interactions and Effects, S. J. Schneider, ed., NBS Quarterly Progress Report to DoE, September.

Plante, E. R. (1980d). In, MHD Materials-Seed/Slag Interactions and Effects, S. J. Schneider, ed., NBS Quarterly Progress Report to DoE, December.

Plante, E. R. (1981). In, MHD Materials-Seed/Slag Interactions and Effects, S. J. Schneider, ed., NBS Quarterly Progress Report to DoE, March.

Plante, E. R. and Cook, L. P. (1978). Seventeenth Symposium on Engineering Aspects of Magnetohydrodynamics, Stanford, CA.

Plante, E. R., Olson, C. D., and Negas, T. (1975). Sixth International Conference on Magnetohydrodynamic Electrical Power Generation, II. P. 211, Washington, DC.

Preston, E. and Turner, W. E. S. (1933). J. Soc. Glass Technol., 17, 122.

Scheil, E. and Stadelmaier, H. (1952). Metallk., 43, 227.

Self, S. A. (1979). "Diagnostic Techniques in Combustion MHD Flows". ibid, Bonnell and Hastie (1979).

Spencer, F. E., Jr. and Orning, A. A. (1973). US Bureau of Mines, RI 7786.

Spencer, F. E., Jr., Hendrie, J. C., Jr., and Bienstock, D. (1975). Sixth International MHD Symposium. Washington, DC, June.

Williams, D. E., Nobile, A. A., and Inman, D. (1977). Trans. Inst. Min. Met., 86C, 35.

---

[*] All NBS reports available from the National Technical Information Service, Springfield, Virginia 22161.

8. Figure Captions

1. Non-equilibrium vaporization effect in the K_2O-Al_2O_3-SiO_2 system. Broken curve represents the pure $KAlSiO_4$ phase. Run chronology for the partially decomposed $KAlSiO_4$ system follows the temperature sequence ABC (KMS data).

2. Selected potassium pressures (KMS data) over synthetic "Western" (W) and "Eastern" (E) channel slags with K_2O compositions (wt.%) of W_2 (19 to 17.6), W_3 (12.9 to 10.8) and E (23.3 to 22.1). "Eastern" slag data points omitted for clarity but they are of similar precision to the "Western" slag data (see Plante and Cook, 1978).

3. Selected potassium and oxygen partial pressure data (KMS) for a synthetic "Eastern" MHD-channel slag with composition (K_2O wt.%) 23.3 to 22.8 (AB interval) and 22.8 to 22.1 (BC interval). Run chronology follows the temperature sequence ABC. Open and closed circles (and solid curves) refer to potassium data, with increasing and decreasing temperaure run-chronology, respectively. Open and closed triangles (and dashed curves) refer to oxygen data, with increasing and decreasing temperature run-chronology, respectively.

4. Comparison of six component synthetic K_2-slag (open circles) with a corresponding four component simplified "Western" slag (solid curve). Data (KMS) expressed in normalized K_2O dissociation pressure product form [$\equiv (A_{K_2O})^{0.4}(P_K{}^2 \cdot P_{O_2}{}^{\frac{1}{2}})^{0.4}$ pure $K_2O(\ell)$].

5. KMS data for variation of K_2O activity coefficient with temperature and composition for the K_1 slag. The numbers, ranging from 0.154 to 0.08, refer to the mole fraction of K_2O remaining in the sample at each measurement point. Runs 1 to 3 were carried out consecutively on the same sample. The open-square data point at 1575 K, run 1, was obtained by TMS with additional O_2 present.

6. Comparison of K_2O dissociation pressure-product data for the MHD plasma (broken curves) and slag (solid curves) phases, with 1 wt.% K_2CO_3 seed. The slag phase is the simplified "Western" slag with K_2O wt.% compositions of 5, 10, and 15.

7. Thermodynamic activities (TMS data) for NaCl and KCl in the K_1 slag-alkali exchange process (see text). The indicated reference state partial pressures were obtained from JANAF (1971).

8. KCl activity data, obtained by KMS, for the NaCl(s)-K_2 slag system. Triangles (open run 1, closed run 2)--data based on KCl pressures. Circles (open run 1, closed run 2)--data based on $(KCl)_2$ pressures. Broken curve data are from Asano et al. (1980) for the system 20 mole % KCl + 80 mole % NaCl.

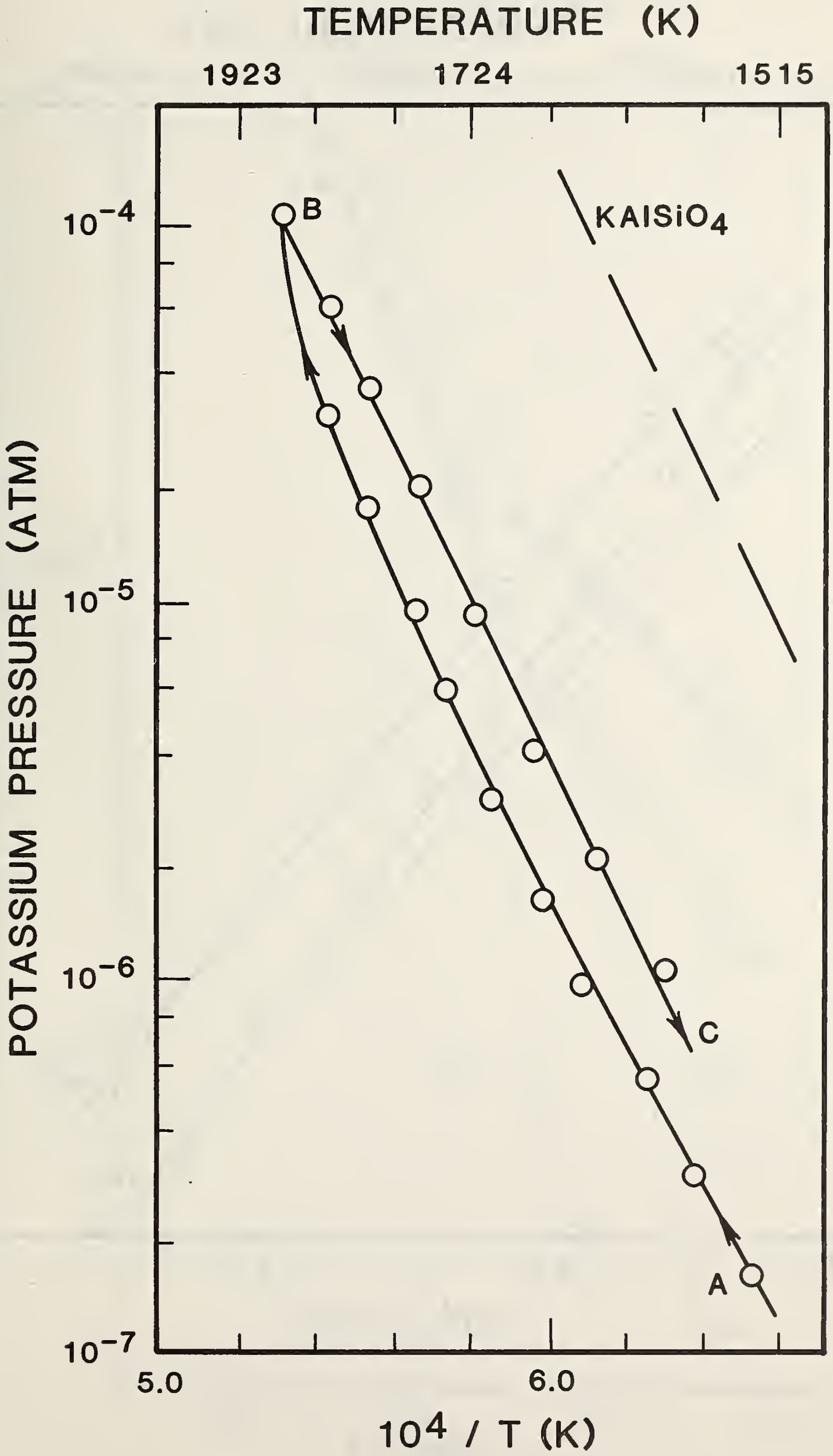
TEMPERATURE (K)
1923
1724
1515
POTASSIUM PRESSURE (ATM)
10^{-4}
10^{-5}
10^{-6}
10^{-7}
B
C
A
$KAlSiO_4$
5.0
6.0
10^4 / T (K)

Figure 1

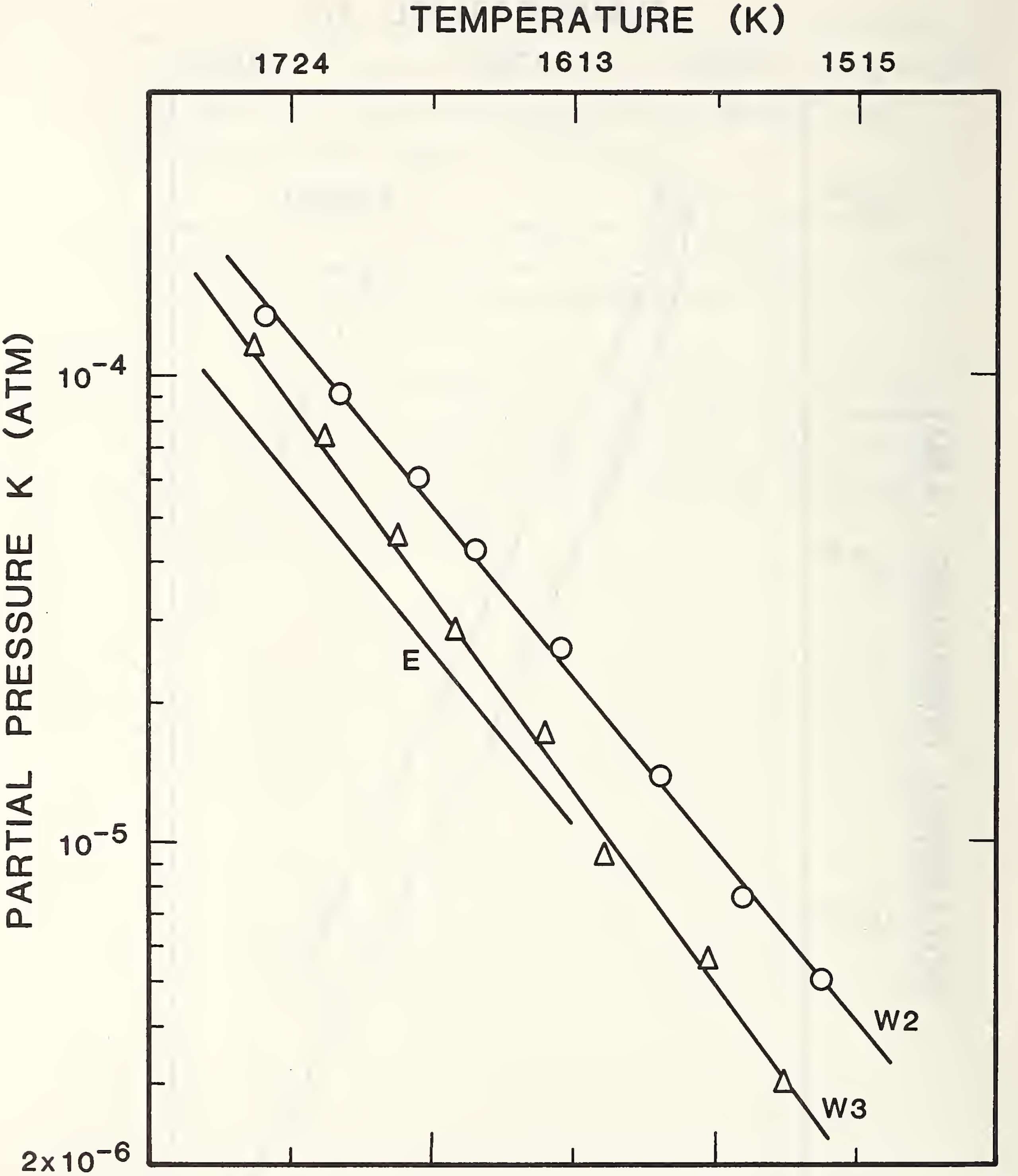
TEMPERATURE (K)
1724
1613
1515
PARTIAL PRESSURE K (ATM)
10^{-4}
10^{-5}
2×10^{-6}
E
W2
W3
5.6
6.0
6.4
6.8
10^4 / T (K)

Figure 2

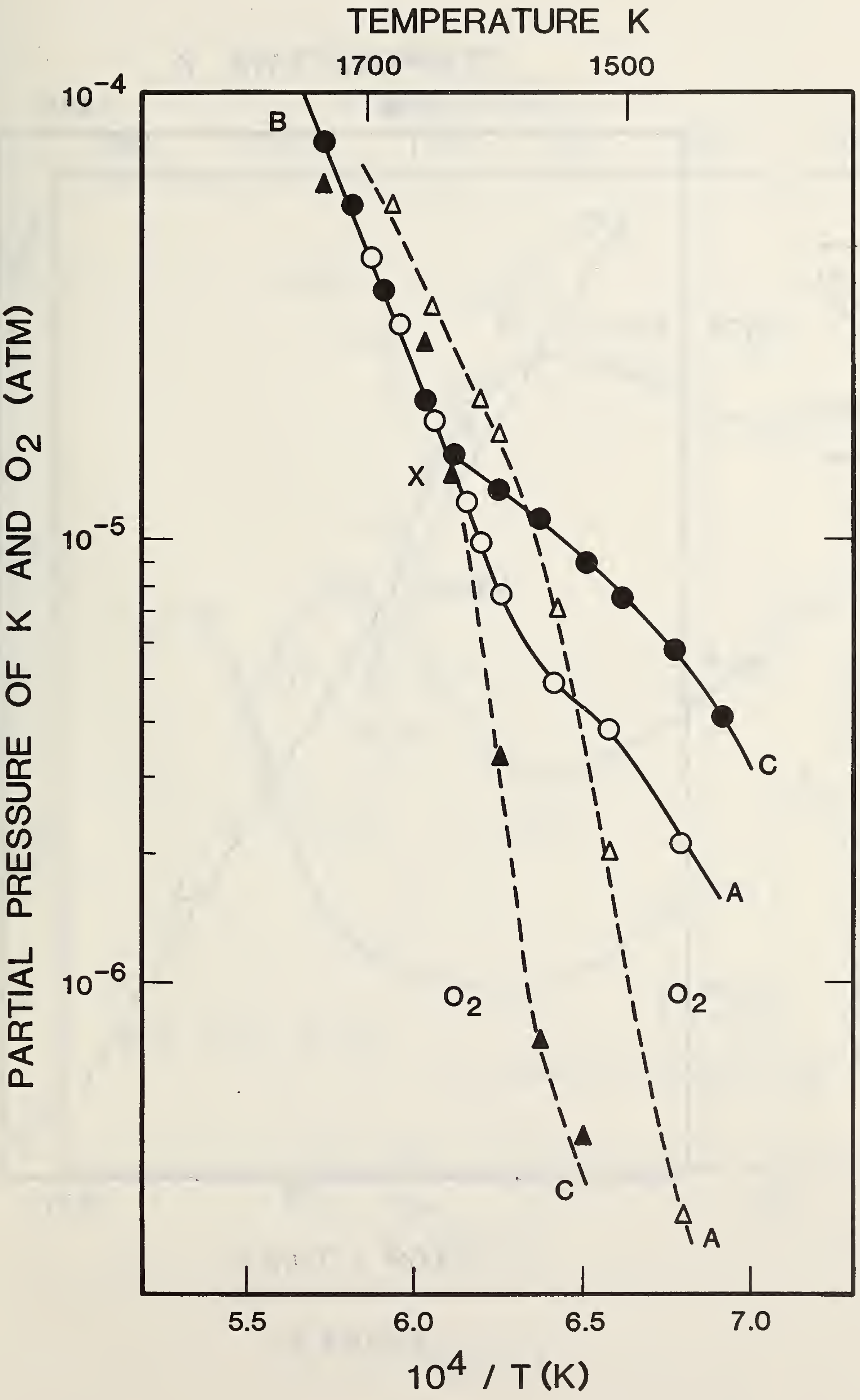
TEMPERATURE K
1700
1500
10^{-4}
10^{-5}
10^{-6}
PARTIAL PRESSURE OF K AND O_2 (ATM)
B
X
C
A
O_2
O_2
C
A
5.5
6.0
6.5
7.0
10^4 / T (K)

Figure 3

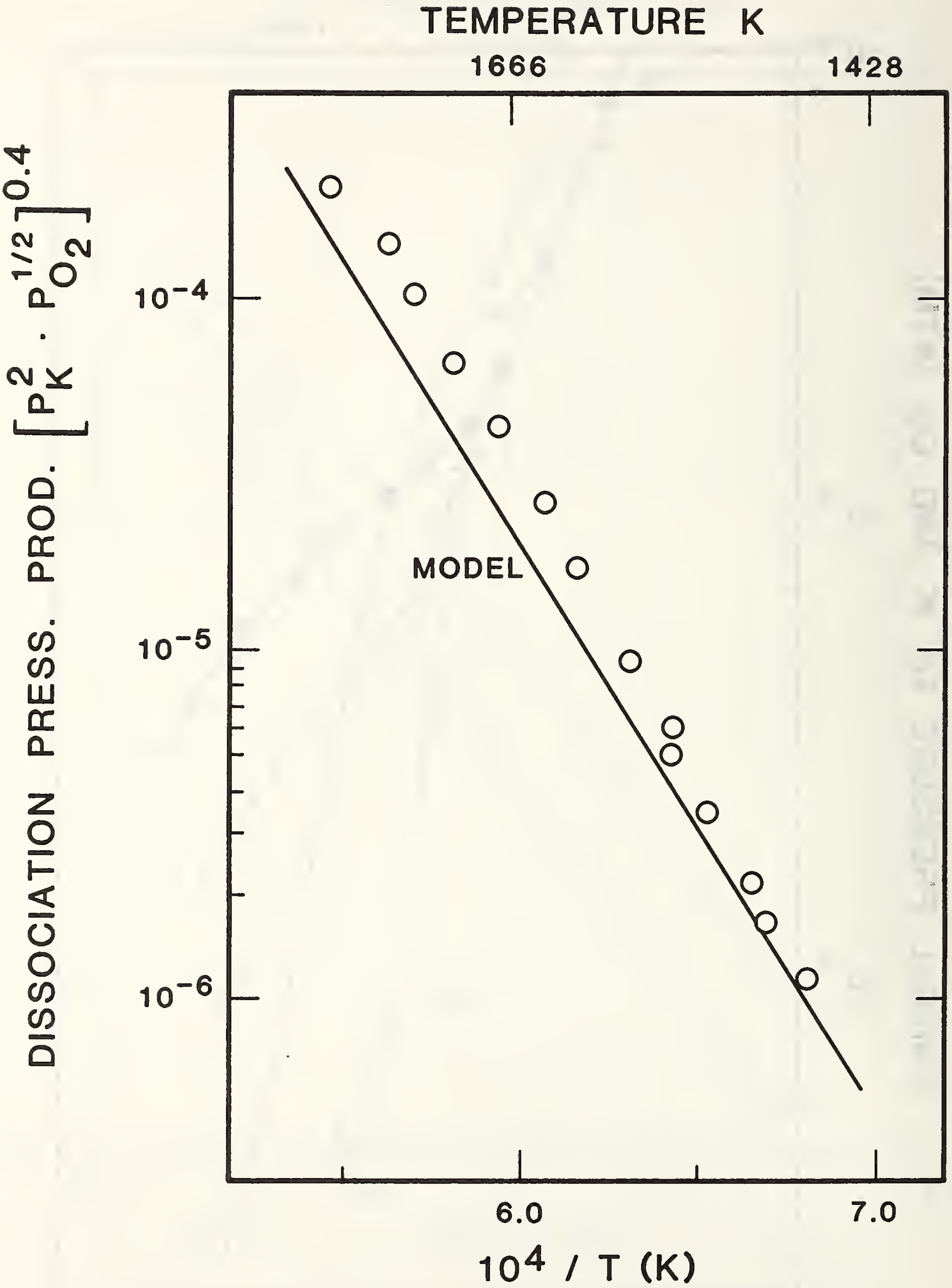
TEMPERATURE K
1666
1428
DISSOCIATION PRESS. PROD. $\left[P_K^2 \cdot P_{O_2}^{1/2}\right]^{0.4}$
10^{-4}
10^{-5}
10^{-6}
MODEL
6.0
7.0
10^4 / T (K)

Figure 4

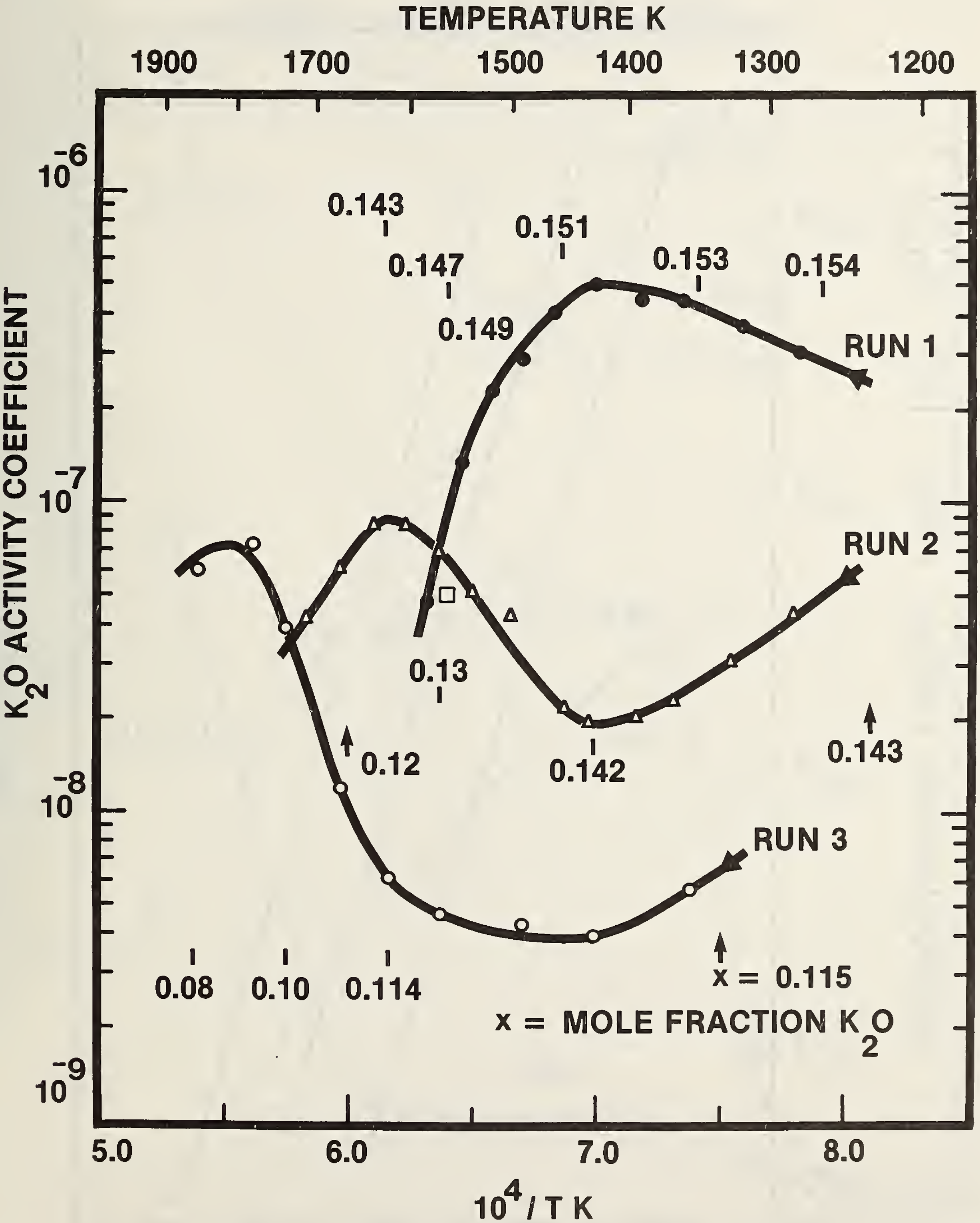
TEMPERATURE K
1900
1700
1500
1400
1300
1200
10^{-6}
10^{-7}
10^{-8}
10^{-9}
K_2O ACTIVITY COEFFICIENT
0.143
0.151
0.147
0.153
0.154
0.149
RUN 1
RUN 2
0.13
0.12
0.142
0.143
RUN 3
0.08
0.10
0.114
x = 0.115
x = MOLE FRACTION K_2O
5.0
6.0
7.0
8.0
10^4 / T K

Figure 5

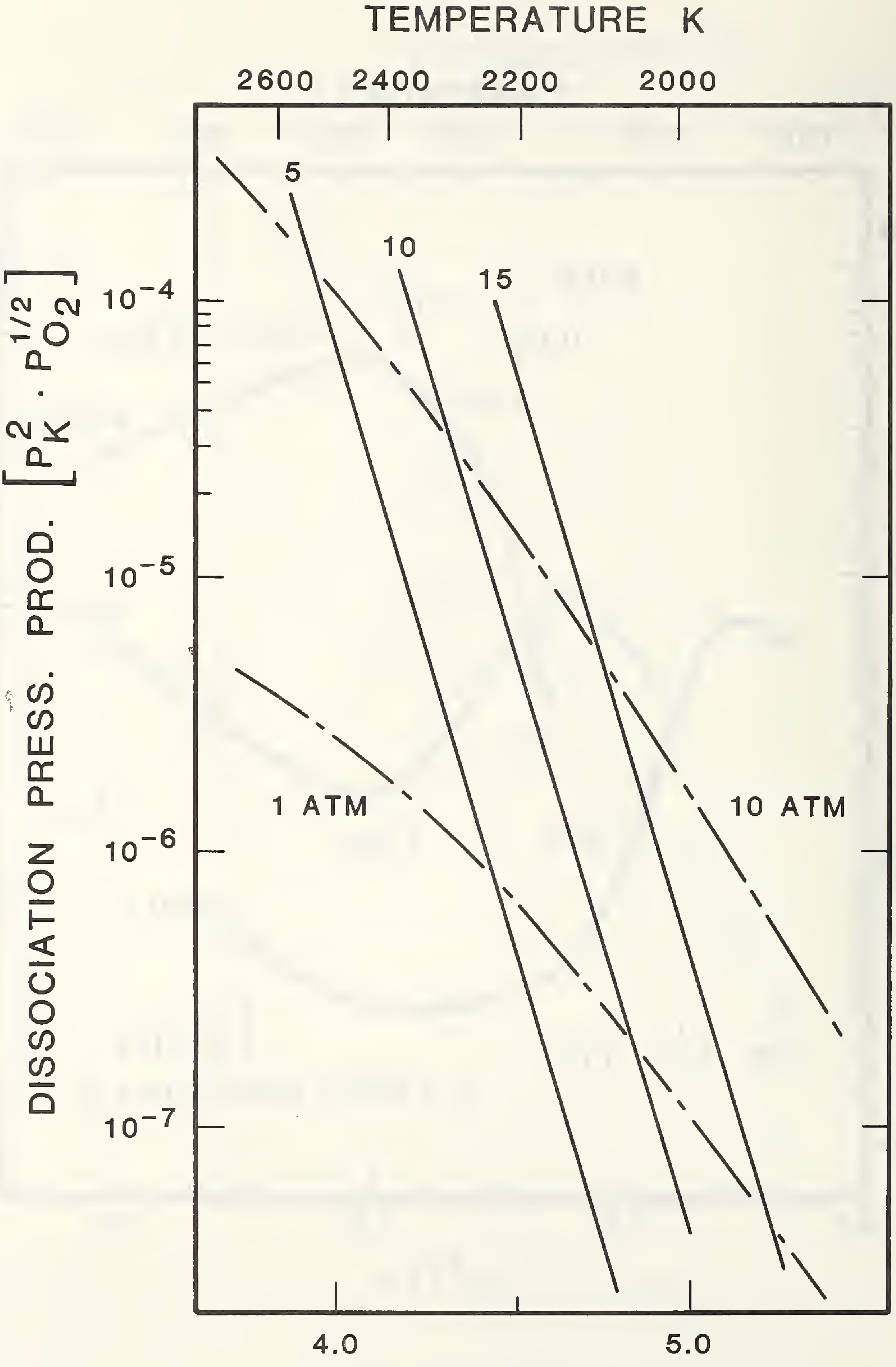
TEMPERATURE K
2600
2400
2200
2000
DISSOCIATION PRESS. PROD. $\left[P_K^2 \cdot P_{O_2}^{1/2}\right]$
10^{-4}
10^{-5}
10^{-6}
10^{-7}
5
10
15
1 ATM
10 ATM
4.0
5.0
10^4 / T (K)

Figure 6

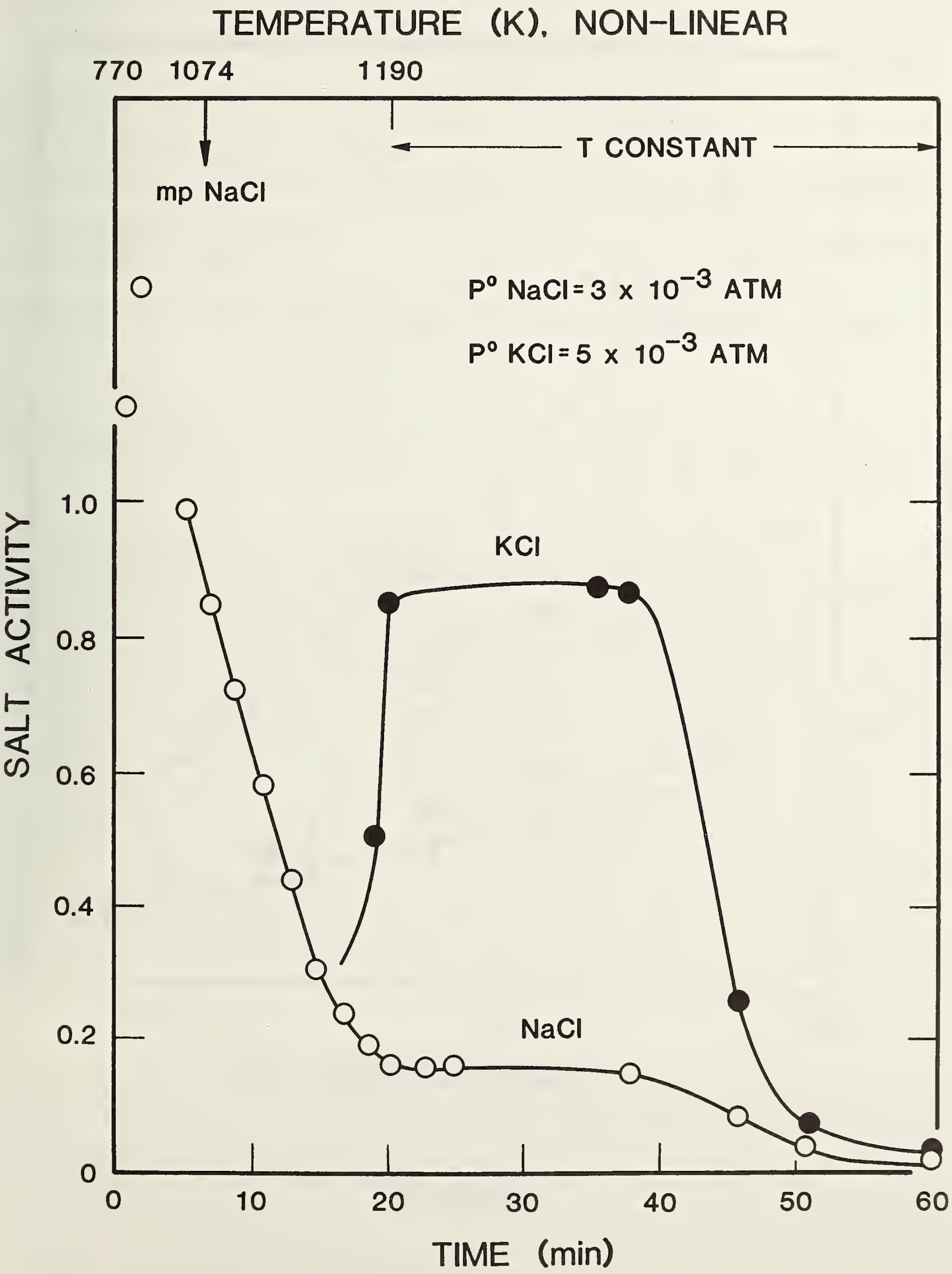
TEMPERATURE (K), NON-LINEAR
770
1074
1190
mp NaCl
T CONSTANT
P^o NaCl = 3 x 10^{-3} ATM
P^o KCl = 5 x 10^{-3} ATM
KCl
NaCl
SALT ACTIVITY
1.0
0.8
0.6
0.4
0.2
0
0
10
20
30
40
50
60
TIME (min)

Figure 7

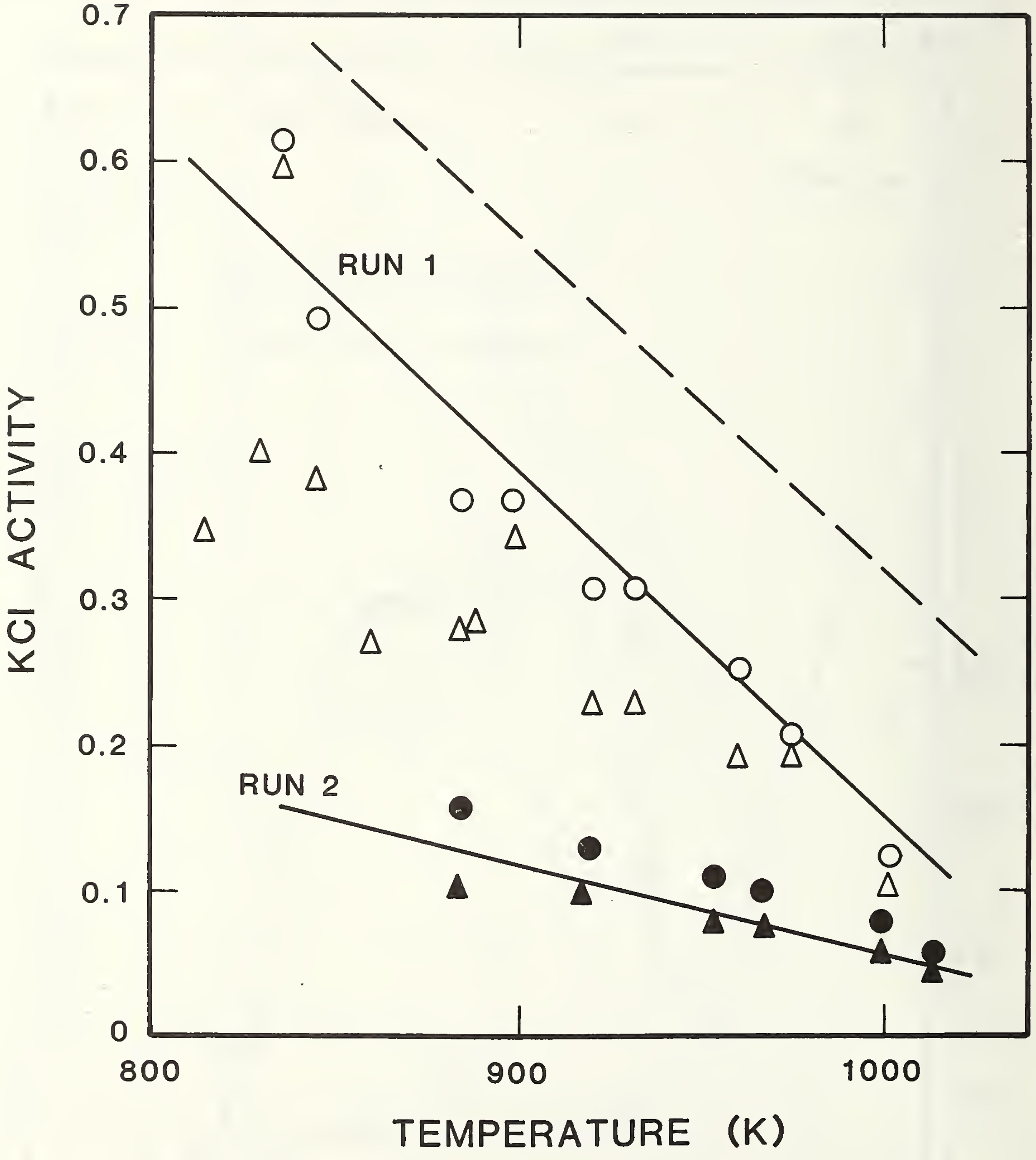
0.7
0.6
0.5
0.4
0.3
0.2
0.1
0
KCl ACTIVITY
RUN 1
RUN 2
800
900
1000
TEMPERATURE (K)

Figure 8

NBS-114A (REV. 2-80)

U.S. DEPT. OF COMM. **BIBLIOGRAPHIC DATA SHEET** *(See instructions)*	1. PUBLICATION OR REPORT NO. **NBSIR 81-2293**	2. Performing Organ. Report No.	3. Publication Date June 1981

4. TITLE AND SUBTITLE

Mass Spectrometric Studies of MHD Slag Thermochemistry

5. AUTHOR(S)

J. W. Hastie and E. R. Plante

6. PERFORMING ORGANIZATION *(If joint or other than NBS, see instructions)*

NATIONAL BUREAU OF STANDARDS
DEPARTMENT OF COMMERCE
WASHINGTON, D.C. 20234

7. Contract/Grant No.

8. Type of Report & Period Covered

9. SPONSORING ORGANIZATION NAME AND COMPLETE ADDRESS *(Street, City, State, ZIP)*

10. SUPPLEMENTARY NOTES

☐ Document describes a computer program; SF-185, FIPS Software Summary, is attached.

11. ABSTRACT *(A 200-word or less factual summary of most significant information. If document includes a significant bibliography or literature survey, mention it here)*

The economic viability of open cycle coal-fired magnetohydrodynamics (MHD) is closely linked to the thermodynamic conditions of seed potassium, both in the plasma and slag phase. Previous attempts to model plasma conductivity and slag retention of seed have been highly inaccurate due to the limited thermodynamic data base available. These limitations have mainly included vapor pressure, enthalpy of formation, and solution activity data for slag phases. Results of an extensive systematic experimental program of measurements on these and related properties are presented. The following potassium-containing systems were studied: binary mixtures of K_2O with SiO_2, Al_2O_3, Fe_2O_3, and ZrO_2; a series of more complex synthetic slags containing K_2O, SiO_2, CaO, MgO, Al_2O_3, and Fe_2O_3; an MHD channel slag (Illinois No. 6 coal); and several slag-NaCl mixtures. Data were obtained over a sufficiently wide range of component-type, composition and temperature to reveal systematic trends in slag activities from which empirical predictions are possible. However, anomalous behavior was also noted, mainly in the form of nonequilibrium effects. Application of the vaporization and activity data to plasma-slag interaction and to the recovery of potassium seed from slag is also considered.

12. KEY WORDS *(Six to twelve entries; alphabetical order; capitalize only proper names; and separate key words by semicolons)*

chemical activity; magnetohydrodynamics; mass spectrometry; potassium slag; thermodynamics; vaporization

13. AVAILABILITY

☒ Unlimited
☐ For Official Distribution. Do Not Release to NTIS
☐ Order From Superintendent of Documents, U.S. Government Printing Office, Washington, D.C. 20402.
☐ Order From National Technical Information Service (NTIS), Springfield, VA. 22161

14. NO. OF PRINTED PAGES

38

15. Price

$6.50